Novel Electrical Dopants for High Performance OLEDs

Dong-Seok Leem, Jae-hyun Lee and Jang-Joo Kim
Department of Materials Science and Engineering and Center for OLEDs,
Seoul National University, Seoul 151-744, Korea
TEL:82-2-880-7893, e-mail: jjkim@snu.ac.kr.

Keywords: **electrical dopants, OLEDs, ReO_3, CuI, Ru_2CO_3**

Abstract

We have developed new electrical dopants of rhenium oxide (ReO_3) and cupper iodide (CuI) as p-dopants and rubidium carbonate (Rb_2CO_3) as an n-dopant, respectively. ReO_3 has advantage of low temperature evaporation (about 300℃) with enhanced device stability. Various kinds of high performance organic light emitting diodes have been realized, including bottom emission, tandem, and top-emission OLEDs.

1. Introduction

Reduction of driving voltage of organic light-emitting diodes (OLEDs) is an important issue to improve the power efficiency in flat panel displays and solid-state lighting applications. One of the most powerful solutions to reduce the driving voltage is to use doping concept in the electron and/or hole transporting layer. Several doping systems based on the organic dopants have been developed up to now. However, their material instability remains to be further enhanced. To overcome the problem, metal oxide-based doping materials such as tungsten oxides (WO_3), molybdenum oxides (MoO_3), and vanadium oxides (V_2O_5) have been introduced recently as *p*-dopants and Cs_2CO_3 as an *n*-dopant. However, their material toxicity and high evaporation temperatures are still problematic for use in conventional OLED processing, which requires further development of other oxide-based doping systems.

In this presentation, we introduce ReO_3 and CuI as novel *p*-dopants and Ru_2CO_3 as an *n*-dopant for high performance OLEDs with *p-i-n* structures. We will demonstrate that the dopants, esp., ReO_3 are superior to conventional MoO_3 in terms of evaporation temperature and charge generation capability by doping. Various types of high performance OLEDs fabricated using the dopants will be presented.

2. Experimental

150 nm-thick-indium tin oxide (ITO) coated glass substrates were prepared and cleaned with solvents. The surface of ITO was treated with UV-ozone for 10 min before depositing organic layers by a thermal evaporator. OLEDs with the *p-i-n* structure were fabricated by successively depositing the 2-8 wt% ReO_3 doped NPB as the *p*-HTL, undoped NPB as the HTL, 8 wt% $Ir(ppy)_3$ doped CBP and 8 wt% $Ir(ppy)_3$ doped Bphen as double emission layers, undoped Bphen as the ETL, and 15 wt% Rb_2CO_3-doped Bphen as the n-ETL on the cleaned substrates, respectively. Tandem OLEDs were fabricated by simply stacking two *p-i-n* single OLEDs with or without a ReO_3 interlayer between the *n/p* junction as an interconnecting charge generation layers. Al was used as the cathode for both devices. Top emission OLEDs have the structure of Ag anode (50 nm)/CuI doped NPB (10 nm)/undoped NPB (10 nm)/CBP:6 wt.% $Ir(ppy)_3$ (25 nm)/BCP (7 nm)/Alq_3 (44 nm)/Yb (1 nm) /Ag (20 nm). 45-nm-thick Alq_3 was deposited as the capping layer to enhance the out-coupling efficiency of the device. The current density-voltage-luminance (*J-V-L*) characteristics of the devices were measured by a Keithley 2400 semiconductor parameter analyzer and a Photo Research (PR-650) spectrophotometer. We measured the angular-dependent electroluminescence spectra by an optical fiber and a S2000 miniature fiber optic spectrometer (Ocean Optics). The absorption and transmittance was measured by means of a UV-Vis-NIR spectrophotometer (Cary 5000).

3. Results and discussion

Low temperature evaporation and high doping efficiency are important characteristics for electrical dopants in OLEDs. Dopant materials with a relatively low evaporation temperature compatible with the common organic materials are strongly required for

practical applications. MoO_3 have been extensively used as the *p*-dopant because it has a lower melting temperature than WO_3 or VO_3. We monitored the evaporation temperatures of two metal oxides of ReO_3 and MoO_3, and NPB as a reference. Two different evaporation cells were used; a low temperature effusion cell operating below 400°C and a high temperature effusion cell operating below 800°C. The results are displayed in Fig. 1. The test with a low temperature cell showed that the evaporation temperature of ReO_3 (0.005 nm/s, doping concentration of 5%) is about 340°C, which is a little

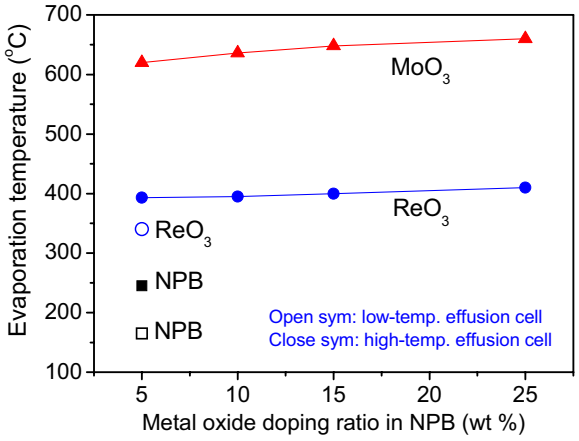

Fig. 1. Evaporation temperature of ReO3 and MoO3 at different evaporation rate in vacuum.

higher than NPB (165°C at 0.1 nm/s). This is the lowest temperature among the oxides applied for the doping system in OLEDs. MoO_3 could not be deposited using the low temperature cell. A high temperature cell can induce re-evaporation of organic materials in the evaporation chamber wall causing cross contamination.

An additional test with a high temperature cell showed that MoO_3 can be deposited in the temperature ranges of 620-660°C. The evaporation temperature of ReO_3 monitored using a high temperature cell was in the ranges of 393-410°C. These results clearly indicate that the evaporation temperature can be significantly reduced by using the ReO_3 compared to MoO_3.

The doping efficiency of ReO_3 and CuI in NPB is compared with MoO_3 in NPB. In general, *p*-doping in a HTL occurs through the charge transfer from the highest occupied molecular orbital (HOMO) of the host material to the lowest unoccupied molecular orbital (LUMO) of the dopant material to form charge transfer (CT) complexes. Therefore, the amount of the CT complexes formed by doping represents the charge generation efficiency of p-dopants. Figure 2 compares the absorption spectra of NPB films doped with ReO_3 and WO_3 and non-doped NPB films. Absorption peaks at the wavelength of 420 and in the range of 1000-2000 nm are originated from the CT complexes. It is clearly seen that the doping of ReO_3 in NPB results in the formation of higher concentration of the CT complexes than MoO_3, indicating that the ReO_3 is more effective in doping than MoO_3. The better doping efficiency of ReO_3 is supposed to be originated from the lower work function of ReO_3 than MoO_3.

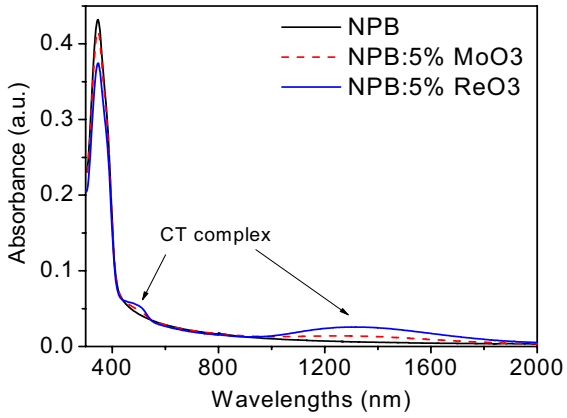

Fig. 2. Absorption spectra of undoped NPB and NPB film doped with MO3 and ReO3.

Effectiveness of doping was further investigated using CuI as a *p*-dopant in various hole transporting materials. Figure 3 shows the

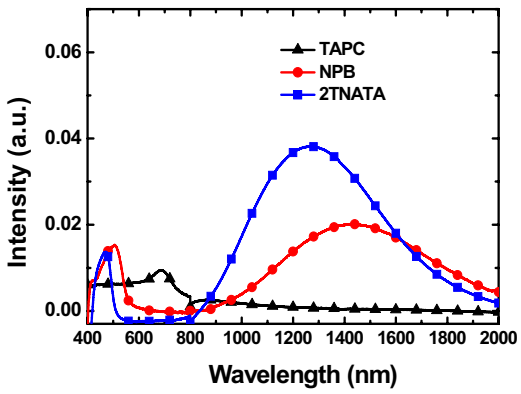

Fig. 3. The difference of absorbance between 20 wt.% CuI doped hole transporting layer (HTL) (50 nm) and undoped HTL (50 nm) for NPB (rectangle), 2TNATA (circle) and TAPC (triangle) as the hole transporting materials, respectively. [3]

difference absorption spectra between CuI doped (20 wt.%) HTL and undoped HTL. Apparently 2-TNATA and NPB films doped with CuI form charge transfer complexes effectively. However TAPC shows little change in absorption by the doping. This behaviour can be easily understood based on the energy levels of the materials. NPB and 2-TNATA have high HOMO level of 5.4 eV and 5.0 eV, respectively. On the other hand TAPC has much lower HOMO level of 5.8 eV. These results indicate that the Fermi level of p-type CuI is located between the HOMO levels of NPB and TAPC, which is consistent with the recent report of the Fermi level of CuI of 5.4 eV.

Various devices were fabricated using the ReO_3 as the *p*-dopant and Ru_2CO_3 as the n-dopant. Doping characteristics of Ru_2CO_3 in Bphen will be reported elsewhere. Figure 4 shows the luminance efficiency and power efficiency of the *p-i-n* OLED with the device structure as the inset. The device with 30 nm thick ETL and 25 nm thick *n*-ETL produced high maximum current efficiency of 65 cd/A corresponding to the external quantum efficiency of 19%. More interestingly the device showed very high maximum power efficiency of 73 lm/W. The high power efficiency was obtained by reducing the driving voltage of the OLED to 3.1 V at 100 cd/m^2 and 3.6 V at 1000 cd/m^2 using the *p*- and *n*-doping [1].

ReO_3 doped NPB/(ReO_3)/Ru_2CO_3 behaves as an effective interconnecting charge generation unit (ICU) in tandem OLEDs. Quantitative analysis of additionally generated charge carriers within the interconnection unit can be performed using the capacitor model shown in the inset of Figure 5. Analysis is performed based on a few assumptions. Firstly, no charges are injected from the electrodes to the devices. It is reasonable because organic layers in the devices are sandwiched by thick insulating LiF layers. Secondly the generated charges are filed up at the interfaces between organic layer/LiF. This assumption is reasonable because the organic layers are thin and the capacitance was measured at 1 kHz. Under the assumptions, we can simply derive the relationship between the amount of internally generated charge density (σ_g) within the interconnection units (ICUs) and capacitance, resulting in the following equation:

$$\sigma_g(V) = \left[\frac{C(V)}{C_0} - 1\right]\left(\frac{d_1/\varepsilon_1 + d_2/\varepsilon_2 + d_3/\varepsilon_3}{d_2/\varepsilon_2}\right)\sigma_0 \quad (1)$$

with

$$C_0 = \frac{\varepsilon_0 A}{d_1/\varepsilon_1 + d_2/\varepsilon_2 + d_3/\varepsilon_3} \quad (2)$$

and

$$\sigma_0 = \frac{C_0 V}{A} \quad (3)$$

where, C is the measured capacitance of sample, C_0 is the capacitance at zero bias, A is the device area, V is the applied bias, and d_i is the thickness of each layer of the ICUs, and ε_i is the effective dielectric constant corresponding to each layer. Figure 5 exhibits the calculated charge density-voltage plots of the ICUs without (ICU A) and with (ICU B) ReO_3 between ReO_3 doped NPB and Ru_2CO_3 doped BCP layer. For both ICUs, the amount of generated charge carriers gradually increases with the increment of applied bias above threshold voltages. It is apparent

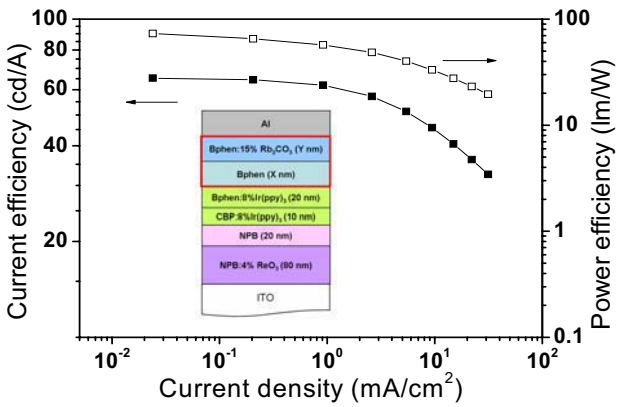

Fig. 4. Luminous efficiency and power efficiency of a *p-i-n* bottom emission OLED as a function of current density. The thicknesses of ETL and *n*-ETL are 30 nm and 25 nm, respectively.

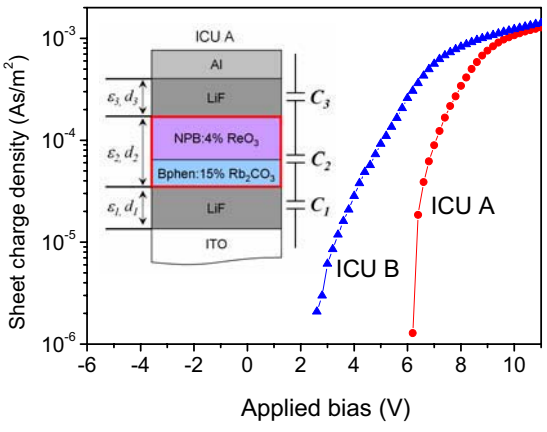

Fig. 5. Interface charge densities as a function of bias voltage of *p-n* junction of LiF/ReO_3 doped NPB/Rb_2CO_3 doped Bphen/LiF structure without (A) and with (B) ReO_3 between the *p*- and *n*- doped organic layers.

that the ICU B begins to generate charges below 3 V which is much lower than the threshold bias of 6 V for the ICU A. These results indicate that addition of a very thin ReO_3 interlayer at the *p-n* junction in the ICU B effectively reduces the voltage to generate charges from ICUs. This efficient charge generation at lower voltage in ICU B lowers the driving voltage and turn-on voltage of the tandem OLEDs compared to those of the tandem OLEDs using ICU A as shown in Figure 6. The devices show very high efficiency of 130 cd/A if ReO_3 is used in the ICUs (ICU B). [2]

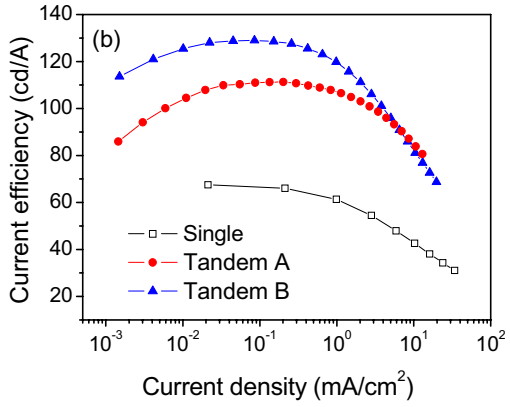

Fig.6. Tandem OLEDs formed by stacking two OLEDs shown in Fig. 4 without (A) and with (B) ReO_3 in the interconnecting unit. [2]

Top emission OLEDs were fabricated on SiO_2/Si substrate and the device structure was described in the experimental section. The fabricated devices were encapsulated prior to the measurement. The maximum current efficiency of 69 cd/A was achieved from the device with the 20 wt.% CuI doped HIL at 0.14 mA/cm^2 as shown in Fig. 7. The efficiency corresponds to the external quantum efficiency of 17.5% as the angular dependence of emission spectrum from the device is Lambertian as shown in the inset of Figure 7, and the spectrum does not change much with emission angle. The current efficiency was enhanced by about 10 % if the glass cap is removed, which will result in 19.3% external quantum efficiency. Roll-off of the efficiency was not significant in the device with the efficiency of 64.6 cd/A at 1000 cd/m^2, and 57.5 cd/A even at 5000 cd/m^2. [3]

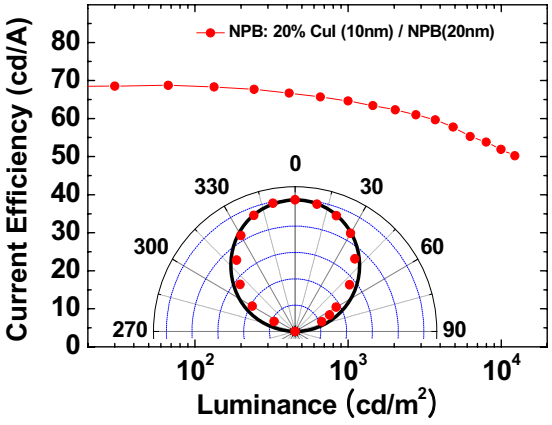

Fig. 7. Luminous efficiency of a top emission OLED employing the CuI hole dopant. [3]

4. Summary

We have developed new electrical dopants of rhenium oxide (ReO_3) and cupper iodide (CuI) as *p*-dopants and rubidium carbonate (Rb_2CO_3) as an *n*-dopant, respectively. ReO_3 has advantage of low temperature evaporation (about 300°C) with enhanced device stability. Various kinds of high performance organic light emitting diodes have been realized, including bottom emission, tandem, and top-emission OLEDs.

5. References

1. Dong-Seok Leem, Hyung-Dol Park, Jae-Wook Kang, Jae-Hyun Lee, Ji Whan Kim, and Jang-Joo Kim, Appl. Phys. Lett. **91**, 011113 (2007)
2. Dong-Seok Leem, Jae-Hyun Lee, and Jang-Joo Kim, Jae-Wook Kang, Appl. Phys. Lett., in print
3. Jae-Hyun Lee, Dong-Seok Leem, and Jang-Joo Kim, Organic Electronics, in print